J Nanostruct 12(3): 761-770, Summer 2022

RESEARCH PAPER

Using ZnO, NiO, and ZnO/NiO as Nano Photocatalyst for Removal of Acid Violet and Rhodamine B from Wastewater

Sajad Jolaei 1, Mortaza Mirzaei [1], Akbar Hassanpour [2]*, Hossein Safardoust-Hojaghan [2], Ali Khani [1]*

[1] *Department of Chemistry, Miyaneh Branch, Islamic Azad University, Miyaneh, I.R. Iran*

[2] *Department of Chemistry, Marand Branch, Islamic Azad University, Marand, Iran*

ARTICLE INFO

Article History:
Received 18 April 2022
Accepted 26 June 2022
Published 01 July 2022

Keywords:
Acid violet
Nanocomposites
Nanoparticles
Photocatalyst
Water pollutant

ABSTRACT

Photocatalyst process as a green method can help significantly remove water pollutants. In his regard, various nanostructures can be applied as a photocatalyst for photodegradation of different dyes. In his work, zinc oxide nanoparticles (ZnO NPs), nickel oxide nanoparticles (NiO NPs), and zinc oxide/nickel oxide nanocomposites (ZnO/NiO nanocomposites) were synthesized through facile and simple co-precipitation route. The polyvinylpyrrolidone (PVP) was applied as a capping agent for controlling of particle size. The crystallinity and morphological properties of prepared products were studied via X-ray diffraction pattern (XRD) and scanning electron microscope (SEM) analysis. The optical band gaps of prepared ZnO NPs, NiO NPs, ZnO/NiO nanocomposites were calculated 3.16 eV, 3.43 eV, and 2.94 eV via UV-Vis-assisted plotting of the $(\alpha h\nu)^2$ versus photon energy ($h\nu$). The obtained products applied as photocatalyst material for phodegradation of acid violet and rhodamine B (RhB). Also, catalyst dosage (0.03, 0.06, and 0.09 g) as an important parameter choose to investigate in the designed photocatalytic process. It is found that prepared ZnO NPs, NiO NPs, and ZnO/NiO nanocomposites shows excellent photocatalytic activity, although ZnO/NiO nanocomposites provided better removal (93.8%) compared to ZnO NPs (86.1%) and NiO NPs (81.5%) toward acid violet. The same trend was observed for rhodamine B. The results confirm that 0.06 g is the optimum dosage of catalyst.

How to cite this article
Jolaei S., Mirzaei M., Hassanpour A., Safardoust-Hojaghan H., Khani A. Using ZnO, NiO, and ZnO/NiO as Nano Photocatalyst for Removal of Acid Violet and Rhodamine B from Wastewater. J Nanostruct, 2022; 12(3):761-770. DOI: 10.22052/JNS.2022.03.029

INTRODUCTION

The ever-developing international concerns about wastewater treatment have performed an vital role in controlling the massive quantity of wastewater and sewage containing a wide style of complicated compositions for the urbanisation and industrialization [1-4]. Even the lower dosage of water pollutants can lead to substantial environment challenges. Therefore, researchers urgently are seeking effective process to obtain pollutant-free water and resolve environmental pollutants troubles [5-7]. So, photocatalytic process as an ecofriendly process can be used to energy conversion and to lead overcoming environmental challenges.

Photocatalysts are determined as substances which decompose adverse materials beneath the sun lighting fixtures containing UV rays [8, 9]. Because photocatalysts have become a feasible

* *Corresponding Author Email: mortazamirzaei_iau@yahoo.com*
hassanpour@marandiau.ac.ir

alternative for pollution control, researchers have labored to enhance their response rate and photocatalytic activity [10, 11]. Due to their attractive applications in free sun power conversion and environmental purification, semiconducting oxide photocatalysts have acquired a number of attention in recent years [12-14]. Whilst water comes into touch with a photocatalyst, it creates hydroxyl radicals (•OH) and superoxide ($•O_2$), that are scavenger radicals. Those scavenger radicals then wreck organic contaminants in a nonselective way, degrading them to smaller, much less poisonous compounds [15]. Till now, the wide range of metal oxide nanoparticles such as CuO [16] , NiO [17], Fe_2O_3 [18, 19], ZnO [20, 21], and TiO_2 [22, 23] have been applied for photocatalytic degradation of water pollutants. Among them, particularly ZnO is the best candidates for its biocompatibility, chemical stability, superior optical properties and economic-competitive photocatalytic activity. But in industrial scale, ZnO nanostructures suffer from some limitations such as low stability, and low rate sunlight harvesting, which is attributed to the absorption of the photons only in the ultraviolet region [24, 25].

For overcoming these restrictions, researchers suggest process includig impurity doping and formation binary compound such as ZnO-based nanocomposites. ZnO-based nanocomposite photocatalysts are found more attention due to their potential for solving global energy supply crises and pollutant degradation [26, 27].

Hosaholalu Balakrishna et al. prepared CuO/ZnO/SnO nanocomposites via electrochemical procedure applying Cu, Zn, Sn and Pt electrode in an aqueous system containing 0.5% $NaHCO_3$ as conductive salt. They characterized prepared samples via XRD, SEM, EDS, TEM, UV-Vis, and PL analysis comprehensively. The crystalline size of prepared nanocomposite was measured 33.7 nm via XRD analysis. The optical band gap was calculated 2.67 eV via Tauc's plot.The photocatalytic efficiency was investigated via photodegradation of acid violet under sunlight. It was found that 94.48% of acid violet degraded after 220 min sunlight irradiation. It was reported that the time o process and amount of catalyst play key role in photocatalytic activity of CuO/ZnO/SnO nanocomposites [28]. Mohammed Abdullah Bajiri et al. prepared CuO/ZnO/g-C_3N_4 through solution combustion route. EDS, TEM, XRD, SEM, and XPS analyses were applied for characterization of products. SEM images exhibited that the obtained nanocomposites have flower-like nanosheets morphology decorated with nanoparticles. The as-synthesized CuO/ZnO/g-C_3N_4 nanocomposites showed better photocatalytic efficiency against acid violet in comparison to the CuO/ZnO nanocomposites under visible light irradiation. At optimum conditions, about 98% of acid violet was removed within 45 min. They found that the excellent photocatalytic performance may be related to the improved redox potential of the CuO/ZnO/g-C_3N_4 nanocomposites and efficient electrons and holes separation induced by the Z-scheme charge carrier transfer [29].

In this work, ZnO NPs, NiO NPs, and NiO/ZnO nanocomposites were prepared via simple co-precipitation route at ambient condition. The prepared samples were characterized via XRD, SEM, FTIR, and UV-Vis analysis. Then the photocatalytic performance of prepared samples were investigated against acid violet and rhodamine B as a water pollutants.

MATERIALS AND METHODS

Synthesis of ZnO NPs

The 3 g of $Zn(NO_3)_2.6H_2O$ was dissolved in the 100 cc distilled water via magnetic stirrer. Then, 2 gr polyvinylpyrrolidone (PVP) was added as capping agent to the solution and stirred for next 30 min. When the solution was clear, the NaOH0.2 M was added dropwise to the solution. The NaOH adding was continued until reaching pH 9. In this stage, the solid was started to formation. After, the NaOH addition was stopped and let the reaction was completed for another 2 h. The solid was filtered and washed twice via distilled water. The obtained solid was dried at 60 ºC for 24 h. Finally, the solid was calcined at 500 ºC for 2 h.

Synthesis of NiO NPs

The synthesis of NiO nanoparticles was similar to the ZnO NPs. Briefly, the 3 g of $NiCl_2.6H_2O$ was dissolved in 100 cc distilled water. After, the 2 g PVP was added. The solid was formed via increasing pH to the 9 via NaOH solution. The solid was filtered and dried for overnight. The dried sample was calcined at 500 ºC for 2 h.

Synthesis of ZnO/NiO NPs

The 3 g of $Zn(NO_3)_2.6H_2O$ and $NiCl_2.6H_2O$ were dissolved in distilled water simultaneously. The 4 g

of PVP was added to the solution under vigorous stirring at ambient condition. After 30 min, the NaOH solution was added to the solution and increased the pH to 9. The NaOH addition was stopped and stirring was continued for next 30 min. Then, the prepared solid was filtered and washed several times via distilled water and ethanol. The solid was transferred to oven and dried for overnight at 60 ºC. The as-prepared solid was heated at furnace for 2h at at 500 ºC.

Characterization

A Philips-X'pertpro X-ray diffractometer was applied to record XRD patterns using Ni-filtered

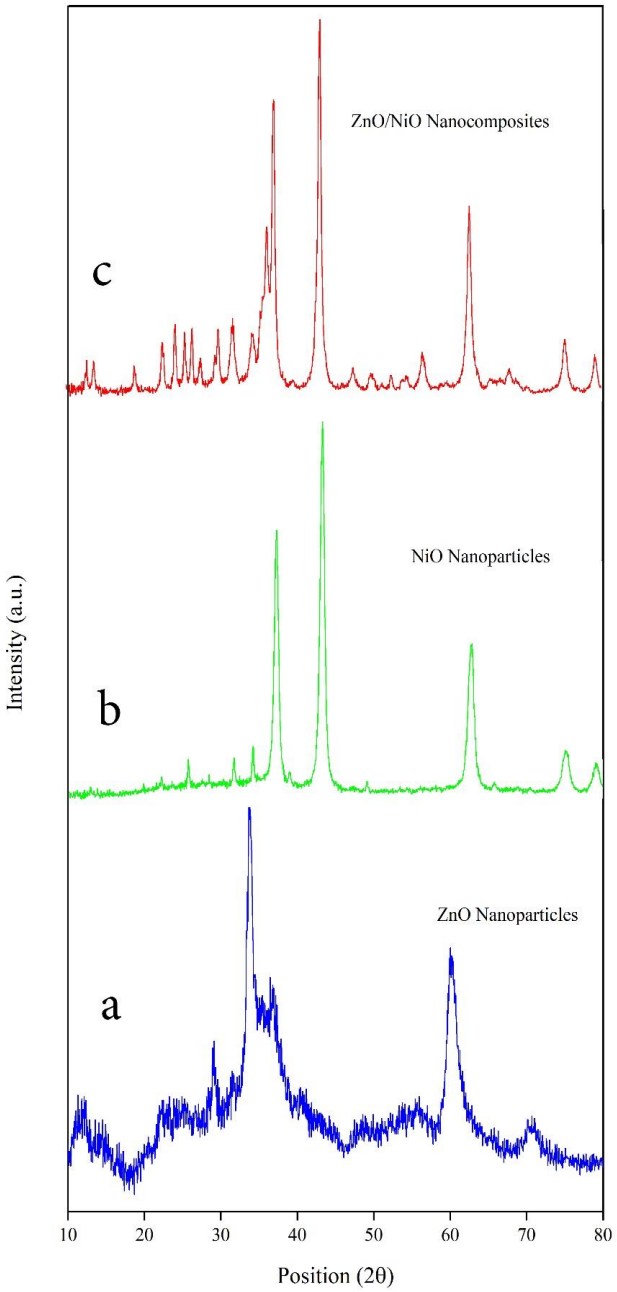

Fig. 1. XRD patterns of prepared a) ZnO NPs b) NiO NPs and c) ZnO/NiO nanocomposites.

Cu K radiation. The LEO-1455VP scanning electron microscope, which was fitted with an energy dispersive X-ray spectroscopy, was used to examine the morphological properties of samples. All of the chemicals used in this study were analytical grade: $NiCl_2.6H_2O$ (99.9%), polyvinylpyrrolidone (PVP), sodium hydroxide(NaOH), and $Zn(NO_3)_2.6H2O$ (99.9%) from Merck.

Photocatalytic test

The photocatalytic performance of prepared NiO NPs, ZnO NPs, and ZnO/NiO nanocomposites were comprehensively studied against of rhodamine B and acid violet. For performing photocatalytic process, 5 ppm concentration of rhodamine B and acid violet were prepared separately. Certain amount of catalysts (0.03 g, 0.06 g and 0.09 g) were dispersed in 50 mL rhodamine B and acid violet solutions. The as-obtained mixture was then stirred in the dark for 30 minutes to performing the adsorption equilibrium of rhodamine B and acid violet on the surface of the prepared catalysts. Then, the xenon arc lamp was turned on for applying UV light to irradiate the mentioned mixture. After every interval of 15 min, 5 mL of the rhodamine B and acid violet solutions were taken out and centrifuged. The light absorbance of the separated solution was examined by an UV spectrophotometer and the concentration of the rhodamine B and acid violet within the solution was measured through the absorbance of UV at the maximum wavelength of rhodamine B and acid violet.

RESULTS AND DISCUSSION

XRD analysis was applied for investigation crystallinity and structural properties of prepared samples. As well as shown in Fig. 1a, the XRD pattern confirms formation of ZnO without impurity. The position of peaks is in good agreement of reference code: 01-075-1533 with hexagonal crystalline structure with space group P63mc and cell constants a = 3.3510 Å, b = 3.3510 Å, and c = 5.2260 Å. For further data, the grain size was determined from Scherrer equation, $Dc = K\lambda/\beta Cos\theta$, where β is the width of the observed diffraction peak at its half maximum intensity (FWHM), K is the shape factor, which takes a value of about 0.9, and λ is the X-ray wavelength (CuKα radiation, equals to 0.154 nm). The crystalline size of ZnO NPs is calculated 26 nm. It was predictable that ZnO nanoparticles had small grain size due to the broad XRD peaks. Fig. 1 b shows the XRD pattern of NiO NPs. The XRD pattern reveals that cubic structure of NiO was formed at reference code: 00-047-1049 with space group Fm3m and cell constant a = b = c = 4.1771 Å. The crystalline size of NiO nanoparticles was measured 19 nm according to Scherrer equation. XRD pattern of ZnO/NiO nanocomposites is displayed in Fig. 1c. The XRD pattern confirms formation of ZnO/NiO nanocomposites without impurity. Broad peaks of XRD pattern relates to the smaller rain size of prepared sample.

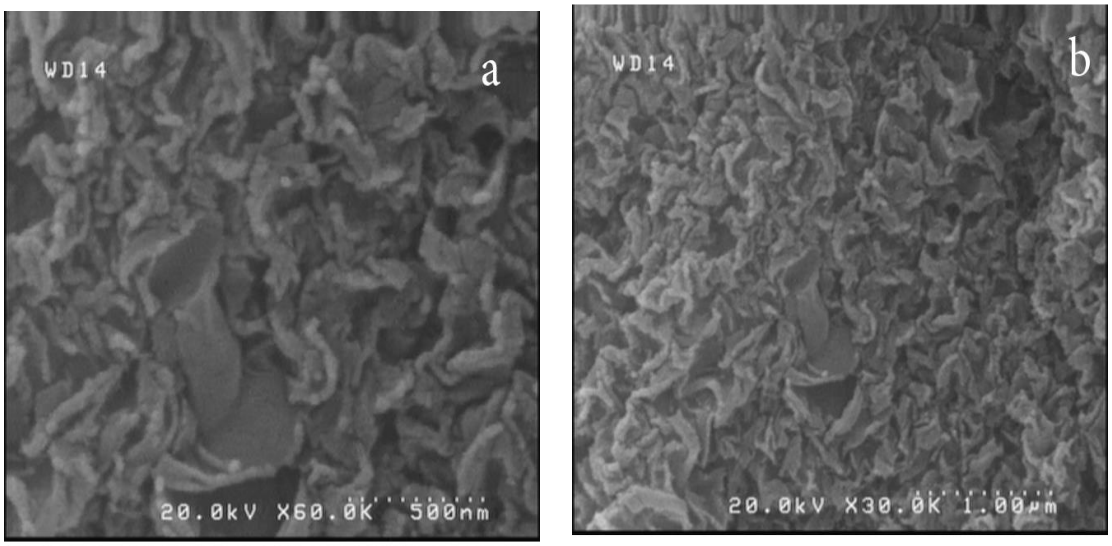

Fig. 2. SEM images of prepared ZnO NPs at two different magnifications.

Scanning electron microscope was applied for investigation morphological properties of prepared nanostructures. Fig. 2 shows the SEM images of prepared ZnO NPs at different magnification. As well as shown the worm-like morphology of ZnO nanoparticles was formed. Interestingly, the

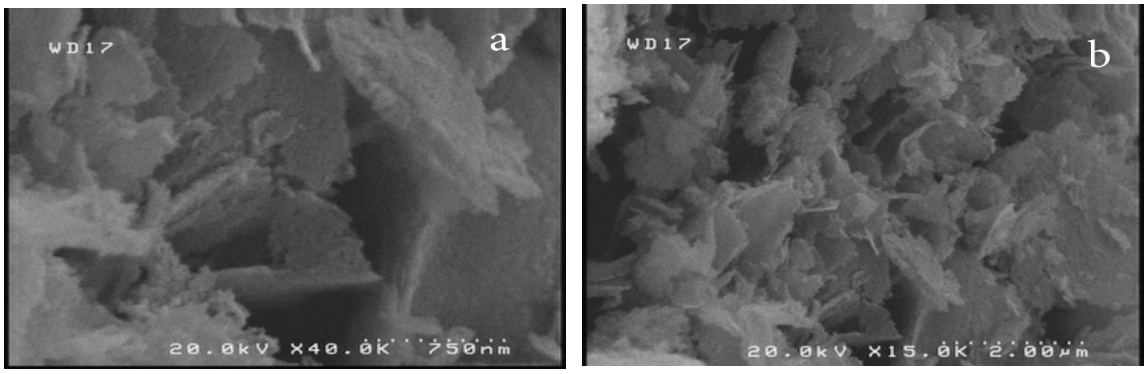

Fig. 3. SEM images of as-synthesized NiO NPs at two different magnifications.

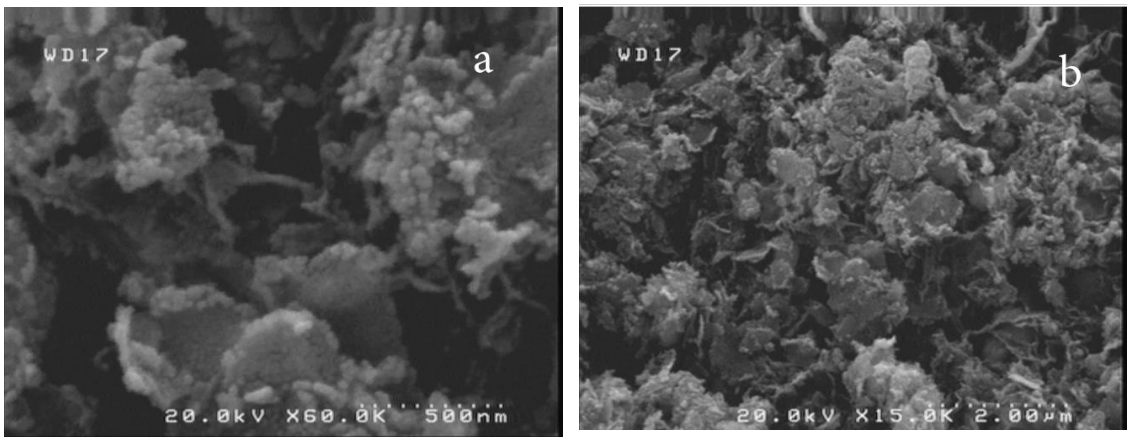

Fig. 4. SEM images of as-prepared ZnO/NiO NPs at two different magnifications.

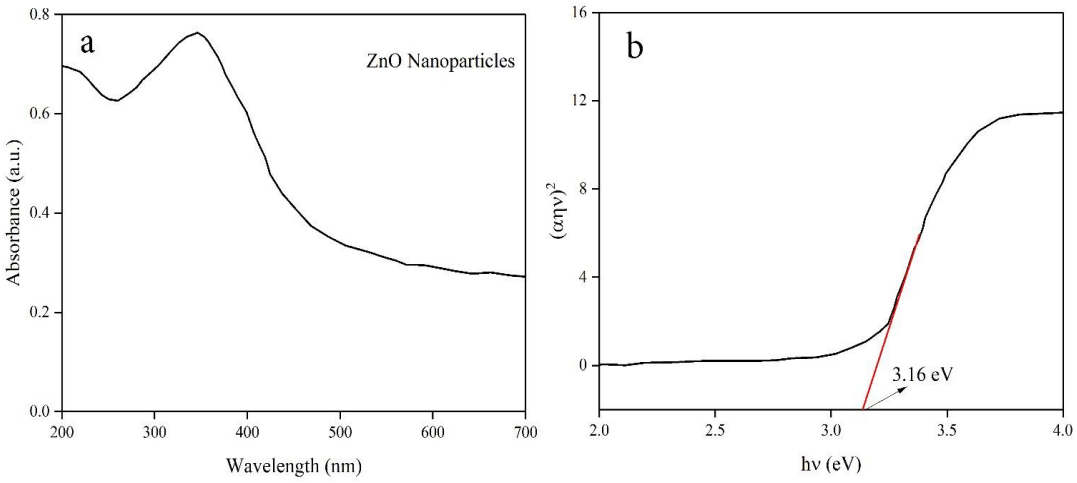

Fig. 5. a) UV-Vis absorption spectra of prepared ZnO NPs b) Measured band gap of synthesized ZnO NPs via plots of the $(\alpha h\nu)^2$ versus photon energy ($h\nu$).

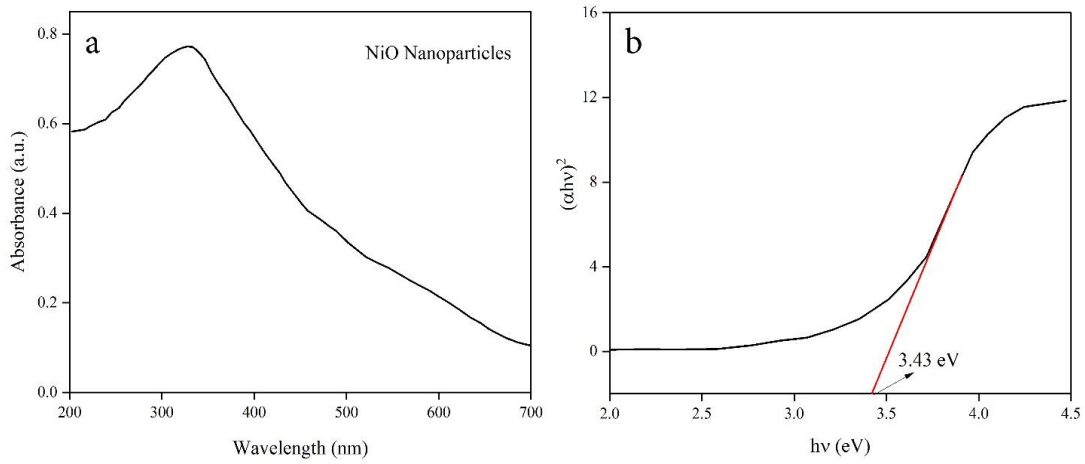

Fig. 6. a) UV-Vis absorption spectra of NiO NPs b) Calculated band gap of NiO NPs via plots of the $(\alpha h\nu)^2$ versus photon energy (hν).

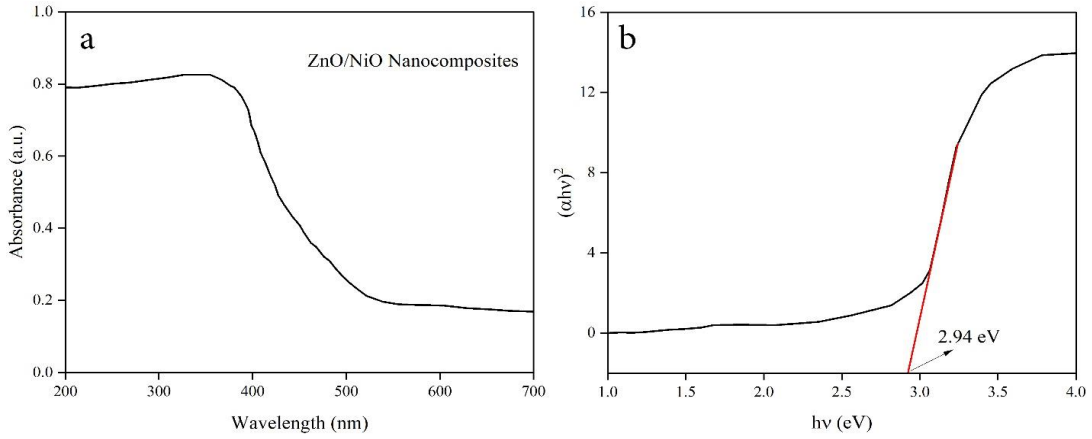

Fig. 7. UV-Vis absorption spectra of ZnO/NiO nanocomposites b) Calculated band gap of ZnO/NiO nanocomposites via plots of the $(\alpha h\nu)^2$ versus photon energy (hν).

worm-like morphology was uniformly formed. The diameter of ZnO nanostructure was determine 47 nm. Fig. 2 b shows agglomeration of particles that due to the higher surface energy of particle at nano scale which lead to linking of particles together. Fig. 3 displays SEM images of prepared NiO nanoparticles. It is obvious that uniform plate-like morphology of NiO is formed. The thickness of plates was calculated 38 nm. Fig. 4 exhibits the SEM images of prepared ZnO/NiO nanocomposites. It is predictable that worm-like morphology of ZnO nanostructures is observable beside NiO nanoplates.

The optical properties of catalysts plays vital role in the photocatalytic process, so the optical properties of prepared ZnO NPs, NiO NPs, and ZnO/NiO nanocomposites were recorded using UV-Vis diffuse reflectance spectroscopy (DRS). Fig. 5a shows UV-Vis diffuse reflectance spectroscopy of prepared ZnO NPs. The Tauc plot was provided via the Tauc equation. As observable, the optical band gap is calculated 3.16 eV via plotting $(\alpha h\upsilon)^2$ vs hυ (Fig. 5b). Fig. 6 shows DRS analysis of synthesized NiO nanoparticles. The band gap of NiO nanoparticles was measured 3.43 eV. For ZnO/NiO nanocomposites, the optical band gap was calculated 2.94 eV. The provided band gaps are superior characteristics for the photodegradation of organic pollutants (Fig. 7).

To study photocatalytic performance of prepared

ZnO/NiO nanocomposites nanocomposite, the photodegradation of acid violet and rhodamine B in aqueous solution under ultraviolet irradiation were performed. When acid violet and rhodamine B mix with synthesized nanostructures under ultraviolet irradiation, decolorization process performs. The photocatalytic efficiency calculates via eq. 2:

$$\text{Photocatalytic efficiency } (\%) = (C_0\text{-}C_t/\ C_0) \times 100$$

Where C_0 (mgL^{-1}) is the initial concentration of acid violet and rhodamine B in solution, and C_t (mgL^{-1}) is the concentration of acid violet and rhodamine B at any irradiation time t (min). Fig. 8a illustrates the photocatalytic efficiency of prepared ZnO NPs against rhodamine B and acid violet. It is found that 86.1% and 79.6% of acid violet and rhodamine B were degraded after 75 min respectively. Fig. 8b shows photocatalytic activity of NiO NPs against rhodamine B and acid violet. The results show that the 81.5% and 77.8% of acid violet and rhodamine B respectively. 93.8% and 87.2% of acid violet and rhodamine B were photodegraded by applying ZnO/NiO nanocomposites (Fig. 8c). The results confirm the excellent performance of ZnO/NiO nanocomposites in decolorization of organic pollutants. The better performance of ZnO/NiO can be attributed to the optical band gap energies that lead to synergistic interaction between CuO and ZnO. This interaction prevents charge

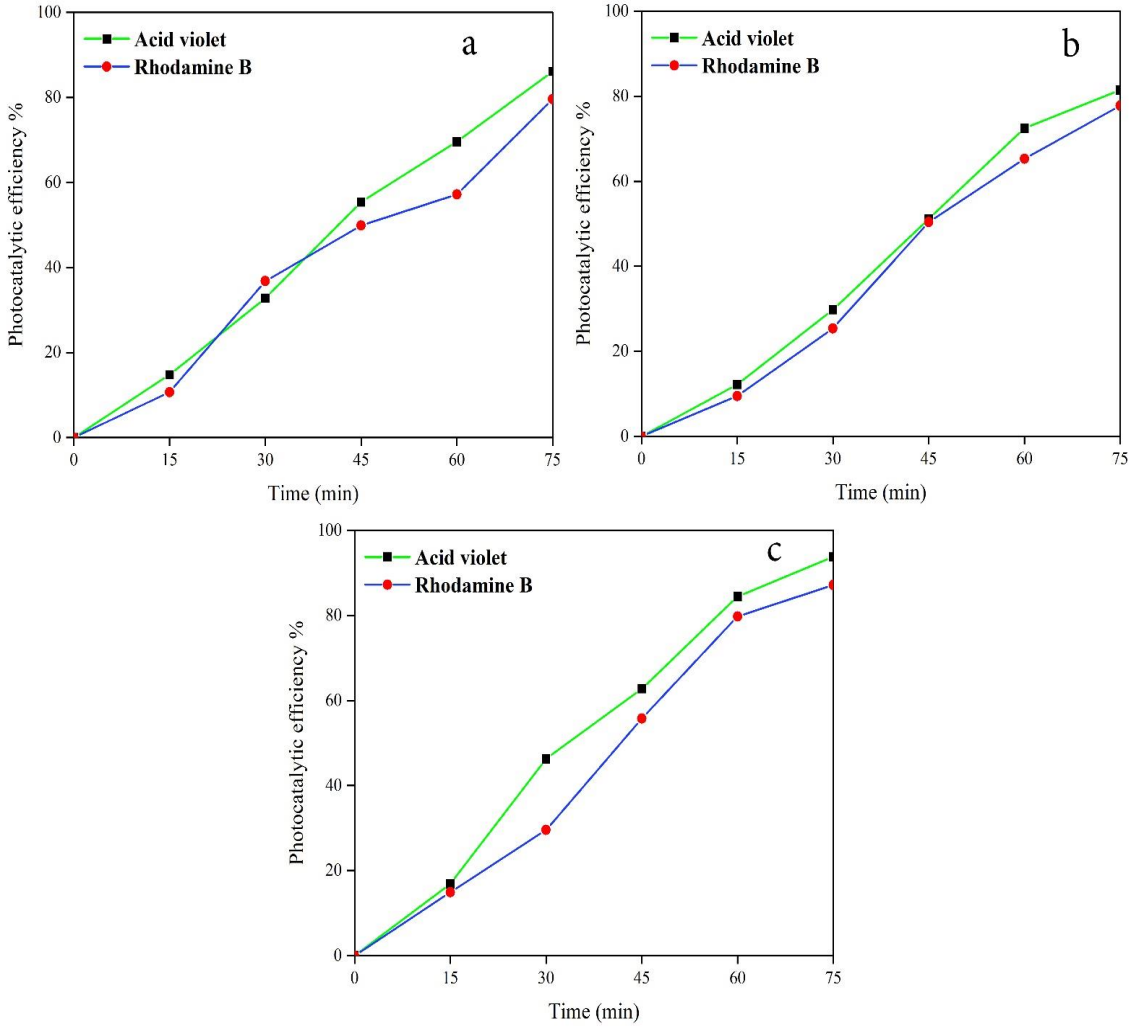

Fig. 8. Photodegradation of acid violet and rhodamine B via a) ZnO NPs b) NiO NPs c) ZnO/NiO nanocomposites under UV irradiation.

$$ZnO/NiO \xrightarrow{h\upsilon} ZnO/NiO\ (e^-_{CB}) + ZnO/NiO(h^+_{VB}) \quad (1)$$

$$O_2 + e^- \rightarrow \bullet O_2^- \quad (2)$$

$$\bullet O_2^- + H^+ \rightarrow \bullet HO_2 \quad (3)$$

$$2 \bullet HO_2 \rightarrow O_2 + H_2O_2 \quad (4)$$

$$H_2O_2 + e^-_{CB} \rightarrow 2 \bullet OH \quad (5)$$

$$h^+_{VB} + H_2O \rightarrow \bullet OH + 2H^+ \quad (6)$$

$$\text{acid violet (rhodamine B)} + \bullet OH \rightarrow \text{Degradation of acid violet (rhodamine B)} \quad (7)$$

recombination and facilitates OH● formation on the surface of ZnO/NiO nanocomposites and accelerates photodegradation process (Reaction 1-7).

Fig. 9 shows the effect of catalyst concentration on the photocatalytic performance of ZnO/NiO nanocomposites. As well as seen, 0.03, 0.06, and 0.009 g of catalyst were applied for photodegradation of acid violet. It is found that the photocatalytic activity is slightly improved via increasing catalyst dosage from 0.03 to 0.06. There is no significant change in photocatalytic efficiency

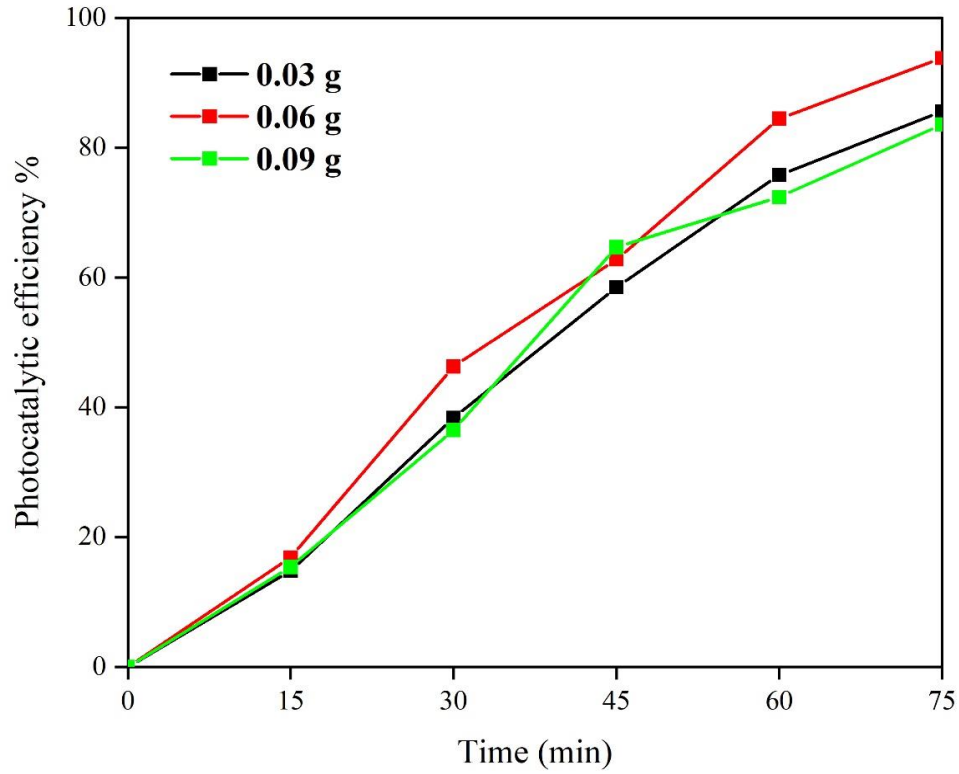

Fig. 9. The effect of amount ZnO/NiO nanocomposites on the photodegradation of acid violet under UV irradiation.

via increasing 0.06 to 0.09. So, it can be concluded that 0.06 is the optimum concentration of catalyst.

CONCLUSION

In conclusion, the ZnO NPs, NiO NPs, and ZnO/NiO nanocomposites were prepared via simple and fast co-precipitation rout. The crystalline structure of prepared samples was characterized via XRD analysis. The grains size of as-prepared ZnO NPs and NiO NPs were calculated 19 and 27 nm, respectively. The morphological properties of prepared samples was investigated via SEM analysis. The optical properties of prepared samples was studied via UV-Vis analysis. The optical band gaps were calculated 3.16, 3.73, and 2.94 eV respectively. The determined optical band gaps lead to application of prepared nanomaterials as a photocatalyst for photodegradation of acid violet and rhodamine B. The results showed that prepared ZnO NPs, NiO NPs, and ZnO/NiO nanocomposites have good photocatalytic properties, although ZnO/NiO nanocomposites showed better efficiency (93.8%) compared to ZnO NPs (86.1%) and NiO NPs (81.5%) toward acid violet. The same trend was observed for rhodamine B.

CONFLICT OF INTEREST

The authors declare that there is no conflict of interests regarding the publication of this manuscript.

REFERENCES

1. Asha S, Hentry C, Bindhu MR, Al-Mohaimeed AM, AbdelGawwad MR, Elshikh MS. Improved photocatalytic activity for degradation of textile dyeing waste water and thiazine dyes using $PbWO_4$ nanoparticles synthesized by co-precipitation method. Environ Res. 2021;200:111721.
2. Coudard A, Corbin E, de Koning J, Tukker A, Mogollón JM. Global water and energy losses from consumer avoidable food waste. Journal of Cleaner Production. 2021;326:129342.
3. Kavitha S, Surendran G, Karunakaran S, Kumari N. Removal of contaminants from waste water by using Murrayakoenigii nanoparticles. Materials Today: Proceedings. 2022;57:1906-1912.
4. Rani S, Chaudhary S. Adsorption of methylene blue and crystal violet dye from waste water using Citrus limetta peel as an adsorbent. Materials Today: Proceedings. 2022;60:336-344.
5. Saravanan A, Senthil Kumar P, Jeevanantham S, Karishma S, Tajsabreen B, Yaashikaa PR, et al. Effective water/wastewater treatment methodologies for toxic pollutants removal: Processes and applications towards sustainable development. Chemosphere. 2021;280:130595.
6. Chatla D, Padmavathi P, Srinu G. Wastewater Treatment Techniques for Sustainable Aquaculture. Waste Management as Economic Industry Towards Circular Economy: Springer Singapore; 2020. p. 159-166.
7. Kanwal M, Tariq SR, Chotana GA. Photocatalytic degradation of imidacloprid by Ag-ZnO composite. Environmental Science and Pollution Research. 2018;25(27):27307-27320.
8. Liang Q, Liu X, Zeng G, Liu Z, Tang L, Shao B, et al. Surfactant-assisted synthesis of photocatalysts: Mechanism, synthesis, recent advances and environmental application. Chem Eng J. 2019;372:429-451.
9. Li L, Salvador PA, Rohrer GS. Photocatalysts with internal electric fields. Nanoscale. 2014;6(1):24-42.
10. Ateia M, Alalm MG, Awfa D, Johnson MS, Yoshimura C. Modeling the degradation and disinfection of water pollutants by photocatalysts and composites: A critical review. Science of The Total Environment. 2020;698:134197.
11. Nowakowska M, Szczubiałka K. Photoactive polymeric and hybrid systems for photocatalytic degradation of water pollutants. Polymer Degradation and Stability. 2017;145:120-141.
12. Rafiq A, Ikram M, Ali S, Niaz F, Khan M, Khan Q, et al. Photocatalytic degradation of dyes using semiconductor photocatalysts to clean industrial water pollution. Journal of Industrial and Engineering Chemistry. 2021;97:111-128.
13. Fang B, Xing Z, Sun D, Li Z, Zhou W. Hollow semiconductor photocatalysts for solar energy conversion. Advanced Powder Materials. 2022;1(2):100021.
14. Al Kausor M, Chakrabortty D. Graphene oxide based semiconductor photocatalysts for degradation of organic dye in waste water: A review on fabrication, performance enhancement and challenges. Inorg Chem Commun. 2021;129:108630.
15. Cruz Santiago LA, Martínez Salazar AL, Vega Moreno J, Reséndiz Hernández O, Portales Martínez B. Fe–Zn–Ti combined systems as photocatalysts for hydroxyl radicals production in sunlight. International Journal of Hydrogen Energy. 2022;47(74):31888-31902.
16. Sibhatu AK, Weldegebrieal GK, Imteyaz S, Sagadevan S, Tran NN, Hessel V. Synthesis and process parametric effects on the photocatalyst efficiency of CuO nanostructures for decontamination of toxic heavy metal ions. Chemical Engineering and Processing - Process Intensification. 2022;173:108814.
17. Lin Z, Du C, Yan B, Wang C, Yang G. Two-dimensional amorphous NiO as a plasmonic photocatalyst for solar H_2 evolution. Nature Communications. 2018;9(1).
18. Mishra M, Chun D-M. α-Fe 2 O 3 as a photocatalytic material: A review. Applied Catalysis A: General. 2015;498:126-141.
19. Hitam CNC, Jalil AA. A review on exploration of Fe_2O_3 photocatalyst towards degradation of dyes and organic contaminants. J Environ Manage. 2020;258:110050.
20. Shekofteh-Gohari M, Habibi-Yangjeh A, Abitorabi M, Rouhi A. Magnetically separable nanocomposites based on ZnO and their applications in photocatalytic processes: A review. Crit Rev Environ Sci Technol. 2018;48(10-12):806-857.
21. Goktas S, Goktas A. A comparative study on recent progress in efficient ZnO based nanocomposite and heterojunction photocatalysts: A review. Journal of Alloys and Compounds. 2021;863:158734.
22. Horikoshi S, Serpone N. Can the photocatalyst TiO_2 be incorporated into a wastewater treatment method? Background and prospects. Catal Today. 2020;340:334-346.
23. Eidsvåg H, Bentouba S, Vajeeston P, Yohi S, Velauthapillai D.

TiO_2 as a Photocatalyst for Water Splitting—An Experimental and Theoretical Review. Molecules. 2021;26(6):1687.
24. Anwer H, Mahmood A, Lee J, Kim K-H, Park J-W, Yip ACK. Photocatalysts for degradation of dyes in industrial effluents: Opportunities and challenges. Nano Research. 2019;12(5):955-972.
25. Iervolino G, Zammit I, Vaiano V, Rizzo L. Limitations and Prospects for Wastewater Treatment by UV and Visible-Light-Active Heterogeneous Photocatalysis: A Critical Review. Topics in Current Chemistry Collections: Springer International Publishing; 2019. p. 225-264.
26. Raizada P, Sudhaik A, Singh P. Photocatalytic water decontamination using graphene and ZnO coupled photocatalysts: A review. Materials Science for Energy Technologies. 2019;2(3):509-525.
27. Johar MA, Afzal RA, Alazba AA, Manzoor U. Photocatalysis and Bandgap Engineering Using ZnO Nanocomposites. Advances in Materials Science and Engineering. 2015;2015:1-22.
28. Uma HB, Ananda S, Kumar MSV. Electrochemical synthesis and characterization of CuO/ZnO/SnO nano photocatalyst: Evaluation of its application towards photocatalysis, photo-voltaic and antibacterial properties. Chemical Data Collections. 2021;32:100658.
29. Bajiri MA, Hezam A, Namratha K, Viswanath R, Drmosh QA, Bhojya Naik HS, et al. CuO/ZnO/g-C_3N_4 heterostructures as efficient visible light-driven photocatalysts. Journal of Environmental Chemical Engineering. 2019;7(5):103412.